

# Processing of full waveform acoustic data

Jean Luc Mari

*Senior Geophysicist and EarthQuick steering committee member*

For many years, the transmission of an acoustic wave through media has been used for borehole measurements. Acoustic logging is an approach to measure the sound propagation velocity in geological formations, using a device composed of a transmitter and a receiver system. Originally, this measurement method, called sonic logging, was essentially intended to measure the interval ( $\Delta t$ ) of arrival times of the first compression wave, with two receivers that are 25 to 50 cm apart, the energy being emitted by a transmitter located about 1 m from the first receiver. A slowness (inverse of velocity) curve is obtained and subsequently used to calculate the propagation velocity of the refracted sonic wave (15 to 30 kHz) in the formations. The use of so-called sonic logging to determine the velocity of compression waves ( $V_p$ ) is a common and relatively well-established practice (Summers and Broding, 1952; Vogel, 1952).

Full-waveform acoustic logging is based on the analysis and processing of the various wave trains (refracted waves, guided waves, reflected waves) recorded by the tool. A geological formation can be simply defined by its elastic parameters from acoustic logging which are P and S velocities ( $V_p$  and  $V_s$ ), density and Q factors of attenuation ( $Q_P$  and  $Q_S$ ). Between transmitters and receivers of the acoustic tool in the borehole, a part of the acoustic

energy propagates in the borehole fluid or mud. A geological formation is said a fast formation if the shear velocity ( $V_s$ ) of the formation is higher than the P-wave velocity in the mud ( $V_p$  fluid). If it is not the case, the geological formation is said a slow formation. Full-wave field recordings mainly enable the determination of the propagation velocities of the different waves.

In the paper we show the benefit of using EarthQuick Software for the picking of arrival times of the different acoustic waves, considering an acoustic section as a seismic section. EarthQuick Software has been developed for the interpretation of seismic sections, mainly based on the picking of seismic horizons and faults.

Figure 1 is an example of a full waveform acoustic logging. The acoustic tool (left image in figure) is a flexible tool with a small diameter and composed of a transmitter and 2 receivers. The distance between the transmitter and the first receiver is 3 m, the distance between the two receivers is 25 cm. The depth reference is ground level. Recording depth corresponds to the depth of the point located halfway between the two receivers. The right side of the figure shows an example of an acoustic section obtained by using a transmitter-receiver pair, 3 m apart. In this representation, the vertical axis represents the depth at which the

sensor is located (3 m in this case), and the horizontal axis represents the listening time (3 ms). The acoustic section is composed of acoustic traces.

Each acoustic trace is the acoustic recording measured by the receiver, which is 3 m from the transmitter, over a listening time of 3 ms. Different wave trains can be identified on the recording.

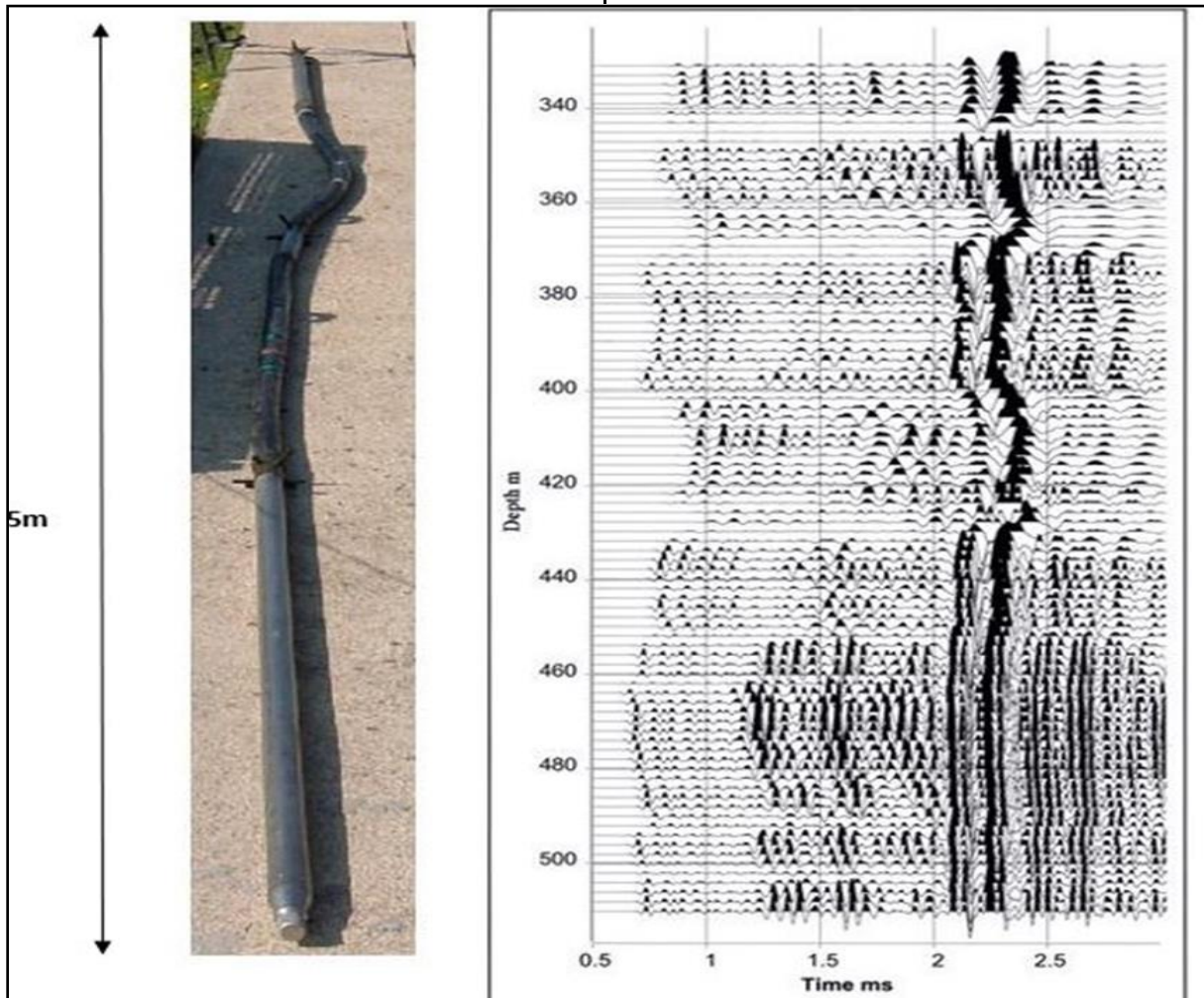


Figure 1: Full waveform acoustic logging – tool and acoustic section.

## Acoustic tools and acoustic waves

Either monopole or dipole tools are used. Monopole tools have multidirectional transmitters and receivers. In the fluid, transmitters generate a compression wave, which creates, in the formation, a compression wave (P-wave) and a shear wave (S-wave) at the refraction limit

angles. Dipole acoustic tools are used to access the S parameters of slow formations and are equipped with polarized transmitters and receivers. Such tools generate polarized compression waves perpendicular to the borehole axis. These compression waves create flexure modes at the well wall that generate pseudo-shear waves in the formation that propagate parallel to the borehole axis.

An acoustic tool is characterized by:

- Type of system:
  - monopole: transmission frequency 10-40 kHz
  - dipole: transmission frequency 1-3 kHz
- Transmitter and receiver type:
  - magnetostrictive
  - piezoelectric
- Number of transmitters and receivers:
  - standard, with one or two transmitters and two receivers
  - receiving antenna with four to eight receivers
- Distance between receivers: from ten to fifty centimeters
- Transmitter offset relative to the first receiver: from one to five meters
- Mechanical characteristics:
  - rigid framework
  - flexible framework
- Time sampling interval:
  - 5 or 10  $\mu$ s for a monopole tool
  - 20  $\mu$ s for a dipole tool
- Listening time:
  - 2 or 5 ms for refracted mode analysis
  - 10 ms or more for reflected mode analysis

Figure 1 left shows a monopole acoustic tool, that is flexible and has a small diameter (50 mm), which is used for geotechnical borehole studies but also for acoustic measurements in the Oil and Gas sector. The transmitter is magnetostrictive (transmission frequencies: 17-22 kHz). It can be equipped with two pairs of receivers (both near receivers (1 - 1.25 m) and far receivers (3 - 3.25 m)).

In a vertical well, monopole tools can enable the recording of five propagation modes:

- Refracted compression wave
- Refracted shear wave, only in fast formations ( $V_s > V_p$  fluid)
- Fluid wave

- two dispersive guided modes, which are pseudo-Rayleigh waves and Stoneley waves:

- Pseudo-Rayleigh waves are reflected conical dispersive waves (Biot, 1952) with phase and group velocities which, at low frequencies (<5 kHz), approach the S velocities of the formation, while at high frequencies (>25 kHz) they asymptotically approach the propagation velocity of the compression wave in the fluid. These waves exist only in fast formations.

- Stoneley waves are dispersive interface waves. In slow formations, they are more dispersive and sensitive to the S-wave parameters of the formation. Stoneley waves are used to evaluate the shear velocity of slow formations, to study

fracturing and to provide an estimation of permeability. At low frequencies, Stoneley waves are analogous to tube waves observed in vertical seismic profile (VSP).

Figure 1 right shows a 3-m constant offset section. The refracted P-wave appears in

the 0.5 - 1 ms range and the Stoneley wave, which have the highest amplitudes, in the 2 - 2.5 ms range. For depths larger than 450 m, the refracted S-wave and the associated pseudo-Rayleigh waves appear in the 1.2 - 2 ms range.

## Processing sequence

Conventional processing of an acoustic log enables time-depth relationship and velocity logs to be obtained at the well, as well as certain mechanical parameters such as the Poisson's ratio.

The processing sequence includes:

1. Editing (elimination of poor-quality recordings).
2. Calculation of acoustic velocities by picking the arrival times of the different wave trains or by velocities scanning and semblance processing.
3. Quality control of velocities (measurement of the correlation coefficient) and of pickings (for example, by flattening the wave train by applying static corrections equal to the picked times).

Comments:

- If the picking algorithm uses a threshold, the detection of erroneous peaks (spikes and cycle jumps) must be done when editing the velocity logs. This technique is only applicable to compression waves.
- If the velocities are measured by semblance, it is recommended to use a tool with a large offset between the transmitter and the first receiver (about 2 to 3 m) and with at least 4 receivers. Measurement is facilitated if the wave trains are well separated in time.

Optional:

1. Measurement of the amplitudes of the different wave trains and calculation of the amplitude and attenuation logs.
2. Measurement of the frequencies of the different wave trains and calculation of the frequency logs (attenuation, resolution...).
3. Calculation of the acoustic porosity (Wyllie's formula or Raymer-Hunt-Gardner equation, ...).

4. Calculation of synthetic seismograms. It is recommended that tying (block shift and minimum  $\Delta t$  methods) of  $\Delta t$  acoustic measurements on VSP measurements is carried out.
5. Calculation of elastic modules (geomechanical: choice of models used).

## Examples of acoustic processing with EarthQuick Software

We show two field examples with acoustic data. The first set of data is obtained with a short-offset acoustic tool. The second set with a large-offset acoustic tool.

### Acoustic logging with a short-offset acoustic tool.

The acoustic data have been recorded in a carbonate formation in the algae limestone (Las Ventanas Formation) located in the Bajo Segura Basin, SE of Spain. The studied geological formation is Las Ventanas Formation, drilled in the northern sector of Bajo Segura Basin with the borehole SB-4. For detailed information concerning the example, the reader is invited to read the paper entitled: Petrophysical characterization of carbonates (SE of Spain) through full-wave acoustic data, written by B. Benjumea, A.I. Lopez, J.L. Mari and J. L. Garcia-Lobon (2019).

The data were acquired with a monopole tool with three receivers spaced 20 cm apart. The offset between the source and the first receiver is 60 cm. Figure 2.a shows the 3 constant offset sections recorded by the three receivers of the acoustic tool (black and grey plots). A color plot of semblance versus tool depth and slowness

( $\mu\text{s}/\text{m}$ ) is displayed in Figure 2.a (Kimball and Marzetta, 1984). First arrival corresponding to the refracted P-wave is characterized by weak amplitude (Figure 2.b) although it is clearly shown in the semblance plot linked to a relative maximum that is shown as red color in the semblance or marked by a red arrow in Figure 2.c as an example for a 90-m depth. The late strong amplitude arrivals identified with a dark blue arrow corresponds to the Stoneley wave. They are characterized by the absolute maximum in the semblance figure. Slowness logs are then converted to velocity logs (Figure 2d). We observe a high correlation coefficient between the 2 velocity logs (0.854). Refracted S-wave is absent in the semblance plot since we cannot identify any secondary maximum between the refracted P-wave and the Stoneley wave arrivals. This means that the shear-wave velocity of the formation is less than P-wave velocity of the borehole fluid which has been defined as slow formation.

### Estimation of formation velocities

We mainly discussed the estimation of velocities by comparing the results obtained by semblance analysis with the results obtained by EarthQuick picking in the reservoir zone located between 107 m and 141 m depth.

We consider only two offset sections noted R1 and R2, with offsets 0.8 and 1.0 m respectively, in the 107 – 141 m depth interval. Figure 3a shows the R1 acoustic section uploaded in EarthQuick software. On the section, we can see the picked times done on the two sections R1 and R2. The curves in green correspond to the picked times of the refracted P-wave on both sections, the curve in red the picked times of the Stoneley wave on section R1, the curve in blue the picked times of the Stoneley wave on section R2. Figure 3b shows a plot of the picked times done on

both sections for the refracted P-wave and the Stoneley wave. The picking has been used to compute the interval velocity logs for both waves. The velocity logs are shown in figure 3c for the refracted P-wave and in figure 3d for the Stoneley wave. For each log, a correlation coefficient log is computed. For that purpose, the section R2 is time shifted to put in phase section R2 with section R1. The time shift value is the difference of travel times for a selected wave (P-wave or Stoneley wave) obtained by picking.

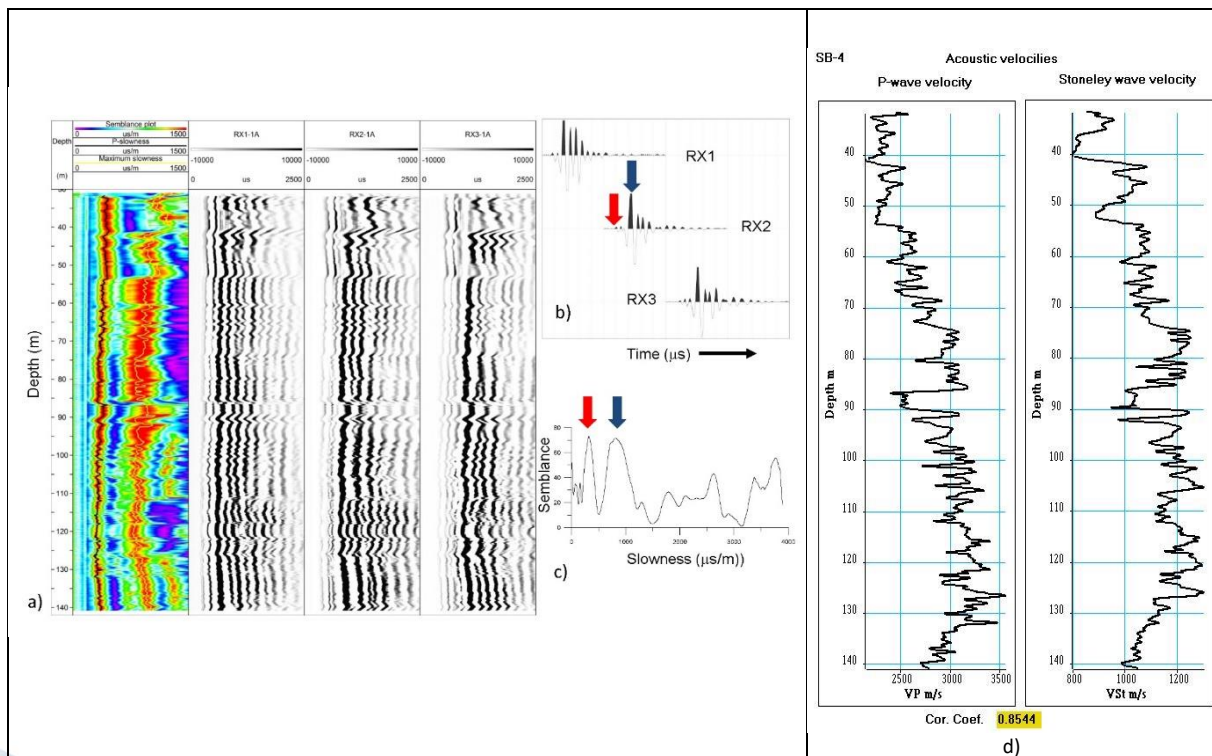
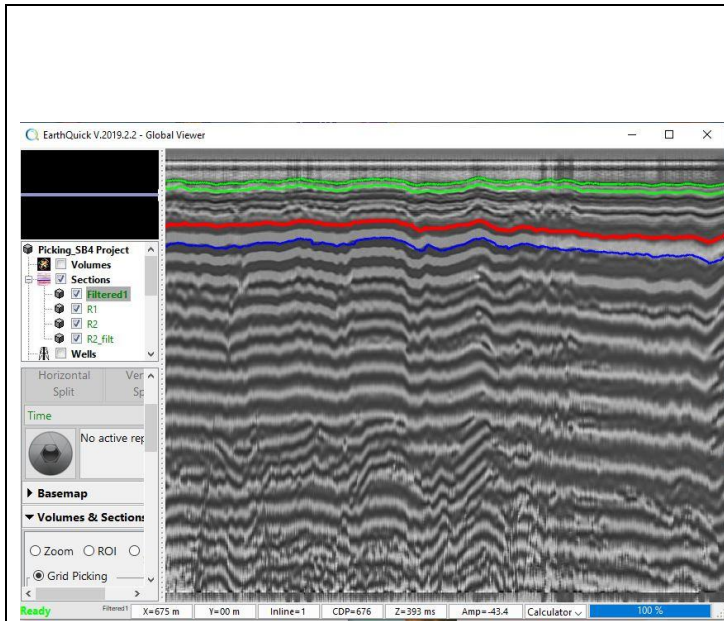
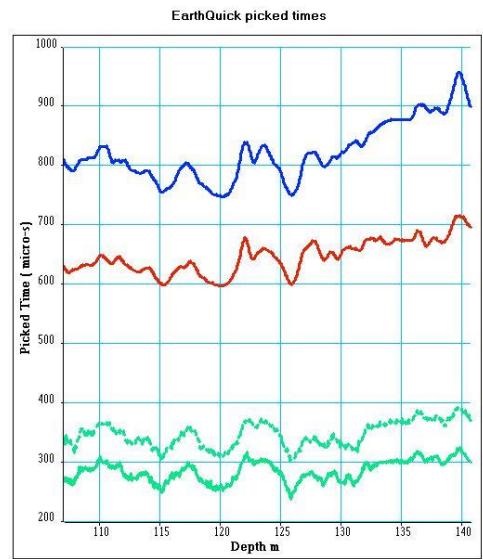


Figure 2: Acoustic logging in slow formation.

- a: Semblance analysis (colored plot) using the seismograms from the three receivers of the FWS probe that are shown in grey scale at each depth. Red indicates high semblance values and blue low semblance values,
- b: Example of wiggle traces of each receiver corresponding to 90 m depth. Red arrow shows P-wave arrival at RX2 receiver and dark blue arrow Stoneley arrivals,
- c: Plot of the semblance value for the seismograms shown in b). Red arrow indicates a semblance maximum corresponding to the P-wave refracted wave while dark blue arrow shows to a semblance maximum related to the Stoneley wave.
- d: P-wave and Stoneley wave velocity logs.

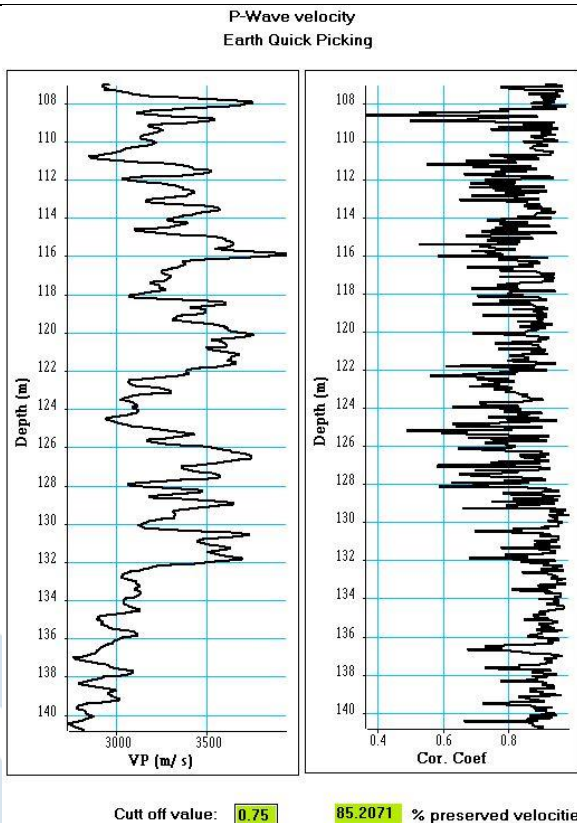


a)

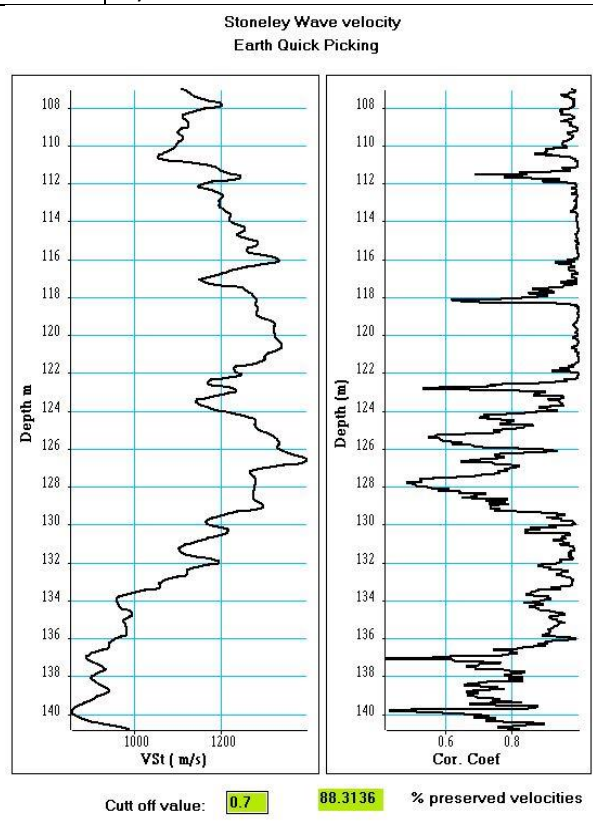


R1 - Offset P-wave picked times: green curve  
 R2 - Offset P-wave picked times: dotted green curve  
 R1 - Offset Stoneley-wave picked times: red curve  
 R2 - Offset Stoneley-wave picked times: blue curve

b)



c)



d)

Figure 3: Velocity logs obtained by EarthQuick picking,  
 a: R1 acoustic section with picked times of P and Stoneley waves,  
 b: Plots of picked times,  
 c: P-wave velocity log and its associated correlation coefficient log,  
 d: Stoneley-wave velocity log and its associated correlation coefficient log.

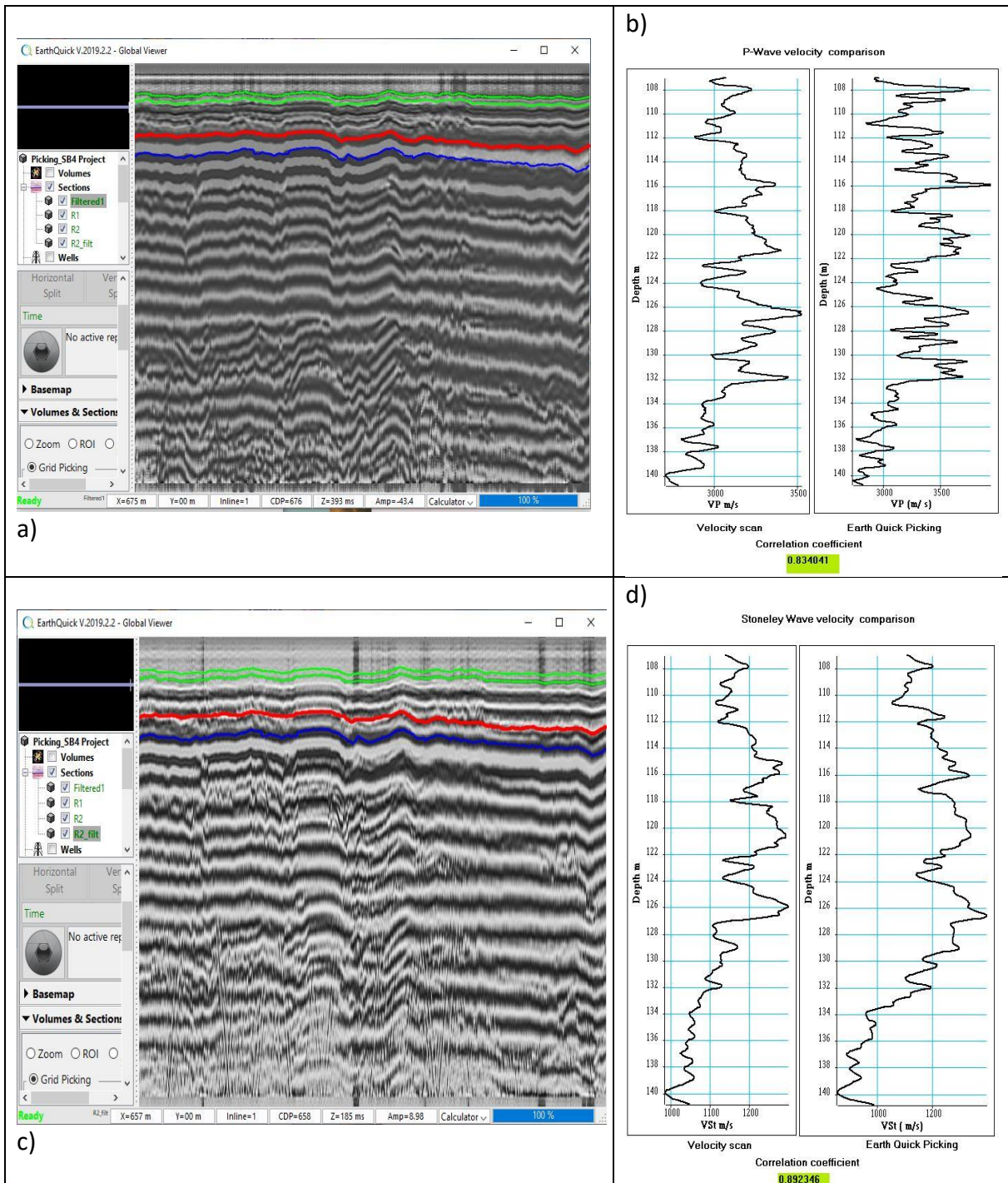


Figure 4: Comparison of velocity logs. EarthQuick picking versus Semblance analysis.  
 a: R1 acoustic section with picked times of P and Stoneley waves,  
 b: comparison of P-wave velocity logs (EarthQuick versus Semblance),  
 c: R2 acoustic section with picked times of P and Stoneley waves,  
 d: comparison of Stoneley-wave velocity logs (EarthQuick versus Semblance).

On a short time-window, the correlation coefficient is computed. High value of correlation coefficient indicates that both shapes of the acoustic signal is the same on

the two receivers (R1 and R2) and the picked times are accurate. A decrease of the correlation coefficient can indicate a poor picking due to either a poor signal to

noise or a change in the signal shape which can be estimated by a qualitative dimensionless attribute: the Shape Index indicator ( $I_c$ ) attribute (Lebreton and Morlier, 1983). The correlation coefficient log can be used to edit the velocity log. If the correlation coefficient is smaller than a given threshold value, the velocity value is cancelled and replaced par linear interpolation. In the example, for the refracted P-wave, with a threshold of 0.75, more than 85 % of the measured velocities is preserved. For the Stoneley wave, a threshold of 0.7 preserves more than 88 % of velocities. The Stoneley wave velocities strongly decrease for depths larger than 128 m.

In the 107 – 141 m depth interval, the velocity logs obtained by EarthQuick picking have been compared with the velocity logs obtained by semblance analysis (velocity scan). The correlation coefficient between the logs is high:  $>0.83$  for the P-wave,  $>0.89$  for the Stoneley wave. The semblance analysis gives a value of velocity averaged on the length of the array of the acoustic tool (here 0.40 m). EarthQuick picking gives a value of velocity over the distance between two receivers (here 0.2 m). Consequently, the velocity logs obtained by semblance are smoother than the logs obtained by EarthQuick. The correlation coefficient between P-wave and Stoneley wave velocity logs is high (0.75) whatever the method used.

#### Some other acoustic parameters

In addition to velocity measurement, the acoustic data can be processed to measure acoustic parameters for each acoustic

wave such as amplitude, attenuation, frequency, distortion of the acoustic signal. The measurements are done on acoustic sections in given time windows. The picked times give the start time of the windows. The attenuation is obtained from the energy ratio of the refracted P-wave, recorded by two adjacent receivers of the acoustic tool, in a time window including the first three arches of the acoustic signal. Frequency is estimated from the difference of transit time between the first and the third arches of the acoustic signal. The acoustic distortion of the refracted P-wave is measured with the Shape Index ( $I_c$ ).  $I_c$  is obtained calculating the ratio  $A_2+A_3$  to  $A_1$  where  $A_1$ ,  $A_2$  and  $A_3$  are the amplitudes of first three arches of the refraction wavelet.  $I_c$  variation indicates the presence of wave interferences, fractures or permeable zones (Mari *et al.*, 2018). Some acoustic attributes computed from the refracted P-wave trains are shown in Figure 5. We can observe an increase of the attenuation associated with a decrease of the velocity below 132 m. The fluctuations of the frequency log are weak. The average dominant frequency is 12.8 kHz for a standard deviation of 0.6 kHz. This is due to the type of transducer which is narrow band. However, we observe a good correlation between attenuation and frequency. The correlation coefficient between the two logs is high:  $>0.73$ . The Shape Index log highlights the abrupt changes of velocity, where the refracted wave can be partly reflected. The interference between the refracted P-wave and the reflected – refracted wave introduces a modification of the shape of the acoustic signal. A peak of Shape Index

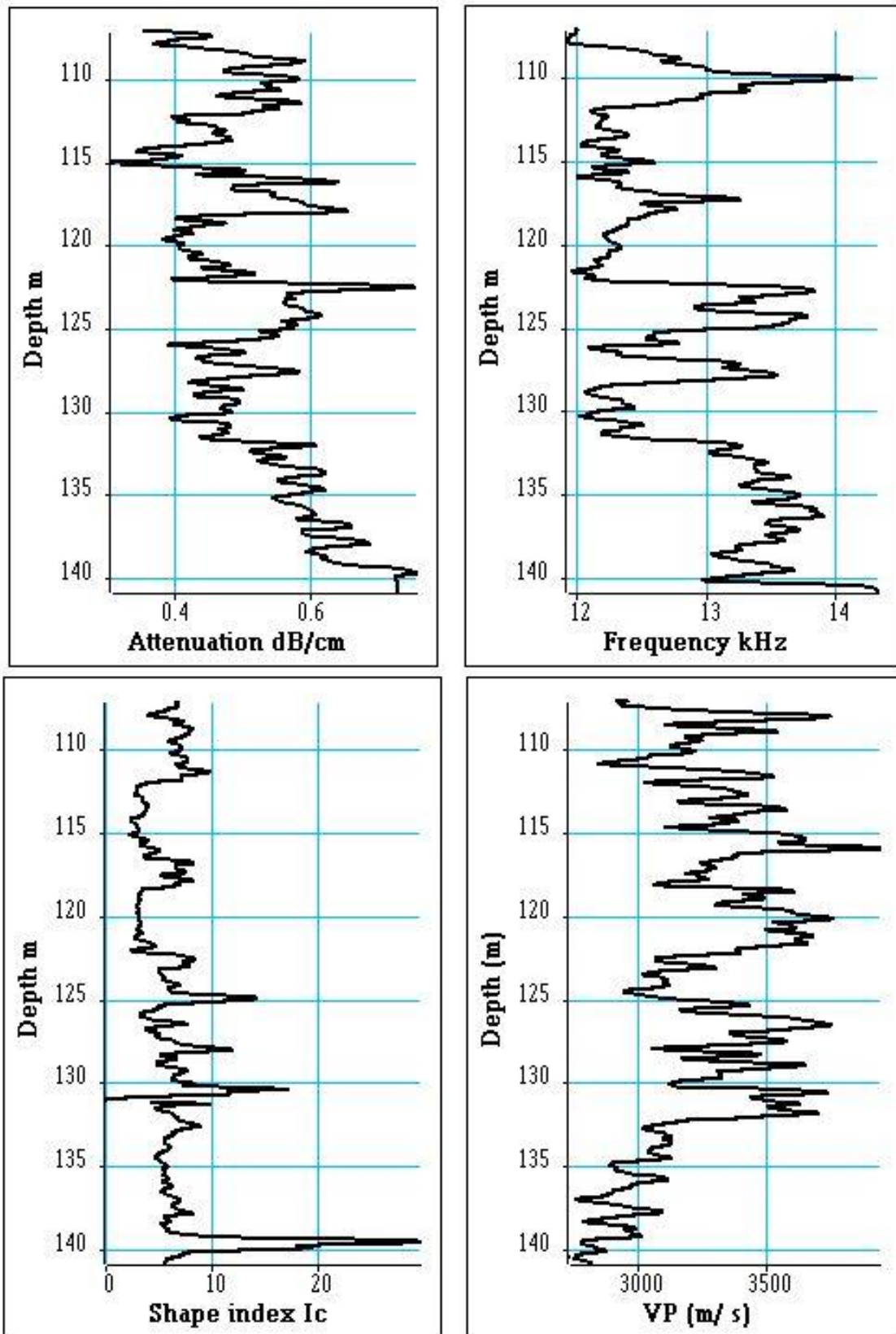


Figure 5: Acoustic attributes from refracted P-wave.

Top: Attenuation and Frequency logs,

Bottom: Comparison between Shape Index  $I_c$  and P-wave velocity  $V_p$ .

associated with a minimum of velocity at 101 m indicates the presence of fractures, confirmed by an ABI log (acoustic borehole imager). At 140 m depth, we observe a peak of the Shape Index which indicates the presence of a highly permeable layer (B. Benjumea et al.,2019).

After calibration, acoustic velocity can be used to predict the porosity of the formation. Here for calibration, we have used the normal short ( $R_{16}$ ) resistivity log to obtain a porosity estimation  $\phi_{RT}$  based on electrical parameters (Archie law):

$$\phi_{RT} = \sqrt{\frac{R_w}{R_{16}}}$$

where  $R_w$  is fluid resistivity that has been set as 2.43 ohm.m.  $R_w$  has been obtained using lab measurements as constraints (26.8 % at 107.3 m, 26.4 % at 118.2 m).  $\phi_{RT}$  log is used as an a priori model to compute a sonic log using the empirical Raymer-Hunt-Gardner law  $\phi_{RH}$  (1980):

$$\phi_{RH} = C \times \left( \frac{\Delta t - \Delta t_{ma}}{\Delta t} \right)$$

where  $\Delta t$  is the measured sonic travel time ( $1/V_p$  expressed in  $\mu s/ft$ ),  $\Delta t_{ma}$  is the theoretical sonic travel time for the matrix, and  $C$  is a calibration coefficient.  $C$  and  $\Delta t_{ma}$  are computed in a root mean square sense to obtain a best fit between the  $\phi_{RT}$  and  $\phi_{RH}$  laws.  $C$  is estimated at 0.72 and  $\Delta t_{ma}$  at 64.59  $\mu s/ft$ . The porosity log  $\phi_{RH}$  is shown in figure 6.

Since the formation is slow, and the acoustic data are recorded with a monopole tool, the shear velocity of the formation  $V_s$  is estimated from Stoneley

wave velocity. According to White (1965),  $V_s$  can be derived from a simplified version of the dispersion equation that relates shear-wave velocity ( $V_s$ ), low-frequency Stoneley velocity ( $V_{st}$ ), formation and fluid and densities ( $\rho$  and  $\rho_f$ , respectively):

$$\frac{1}{V_{st}^2} - \frac{1}{V_f^2} = \frac{\rho_f}{\rho} \cdot \frac{1}{V_s^2}$$

An estimation of  $\rho$  has been done from the Willy equation using both P-wave matrix velocity  $V_{Pma}$ , computed from  $\Delta t_{ma}$ , and porosity:

$$\begin{aligned} \rho &= \rho_{ma}(1 - \Phi) + \Phi\rho_f \text{ with } \rho_{ma} \\ &= \alpha V_{Pma}^\beta \end{aligned}$$

The  $\alpha$  and  $\beta$  Gardner coefficients have been adjusted, using the two previous equations to obtain  $\rho$  and  $V_s$  under the following constraints:

- $V_s$  lower than fluid P-wave velocity (1500 m/s)
- Poisson's ratio must range between 0.3 and 0.5 (for marls and unconsolidated formations).

In this study,  $\alpha$  has been fixed to 0.305 and  $\beta$  to 0.25.

Figure 6 shows the density log, the shear wave velocity log and the Poisson's ratio log.

The contribution of full-wave acoustic logging to permeability estimation is discussed deeply in the reference paper (B. Benjumea et al.,2019).

### Mechanical parameters

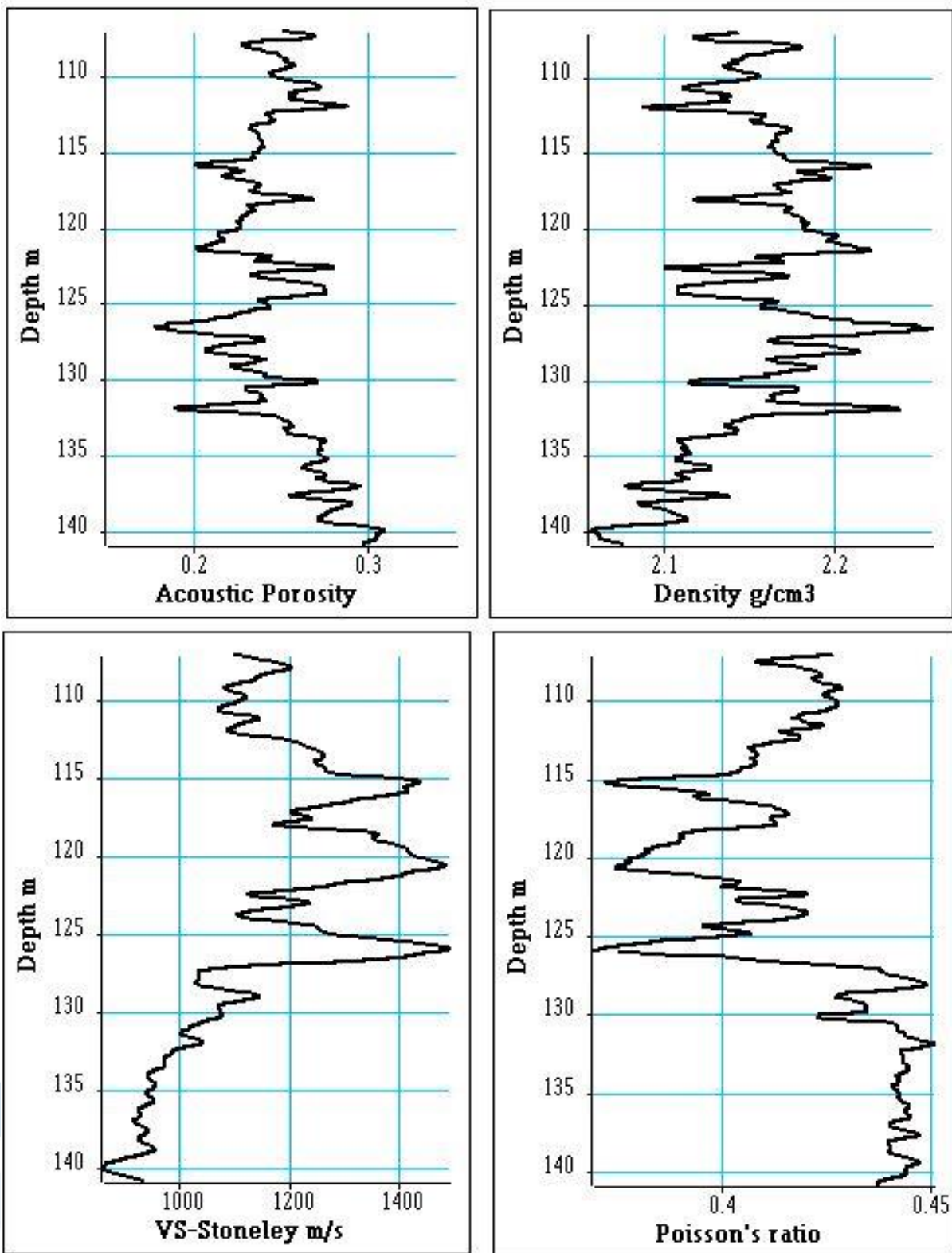


Figure 6: Mechanical parameters

Top: acoustic porosity and density logs,

Bottom: Shear velocity from Stoneley velocity and Poisson's ratio.

## Acoustic logging with a large offset acoustic tool.

Andra (Agence nationale pour la gestion des déchets radioactifs - National Agency for Radioactive Waste Management) conducted a geological survey campaign covering a 250 km<sup>2</sup> zone at the boundary of the Meuse and Haute-Marne departments, in eastern France. One of the drilling platforms was used to study formations ranging from the Oxfordian (Jurassic) to the Trias. The analysis presented here deals with borehole EST431 and covers the Oxfordian formation. For detailed information concerning the example, the reader is invited to read the paper entitled: Characterization of geological formations by physical parameters obtained through full waveform acoustic logging written by Mari, J.L., Gaudiani, P. and Delay, J. (2011).

The acoustic tool used for the field experiment described is a flexible monopole tool with two pairs of receivers: a pair of near receivers (1 and 1.25 m offsets) and a pair of far receivers (3 and 3.25 m offsets). The source is a magnetostrictive transducer. The receivers are independent, and each receiver has its own integrated acquisition device. The data have been recorded through the far offset configuration. The sampling depth interval is 10 cm. The sampling time interval is 5 microseconds. The length of recording is 5 ms.

Figure 7 left shows the 3-m constant offset section (R1) in the 333 – 510 m depth interval. On the acoustic section, the refracted P-waves appear in the 0.6 – 1.2

ms time interval, the converted refracted shear waves in the 1.2 – 2 ms time interval, and the Stoneley wave in the 2 – 2.4 ms time interval. On the acoustic section, we can differentiate:

- An event at 345 m showing a very strong attenuation of all the waves,
- An interval showing a very strong diminution of the P and S waves (360 – 375 m),
- A relatively homogeneous mid-level interval (375 – 397 m),
- A level standing out for its strong variations in P, S and Stoneley velocities (397 – 462 m),
- A very homogeneous zone below 495 m, with easily identifiable P and S waves, and an image of alteration between 501 and 507 m.

In the 342 – 347m depth interval, the acoustic waves are strongly attenuated. After an amplification which compensates the attenuation, we can see that the refracted waves interfere with the reflected-refracted waves. The reflected-refracted waves conventionally named criss-cross events are associated with strong acoustic impedance discontinuities indicating a strong change of the physical parameters (velocity, attenuation, etc.) of the geological medium. A zoom of this zone is shown in figure 7 right.

The arrival times of the different wave trains (refracted P-wave, converted refracted shear wave, Stoneley wave) have been picked using the EarthQuick Software. The results are shown in figure 8 for the two far-offset sections.

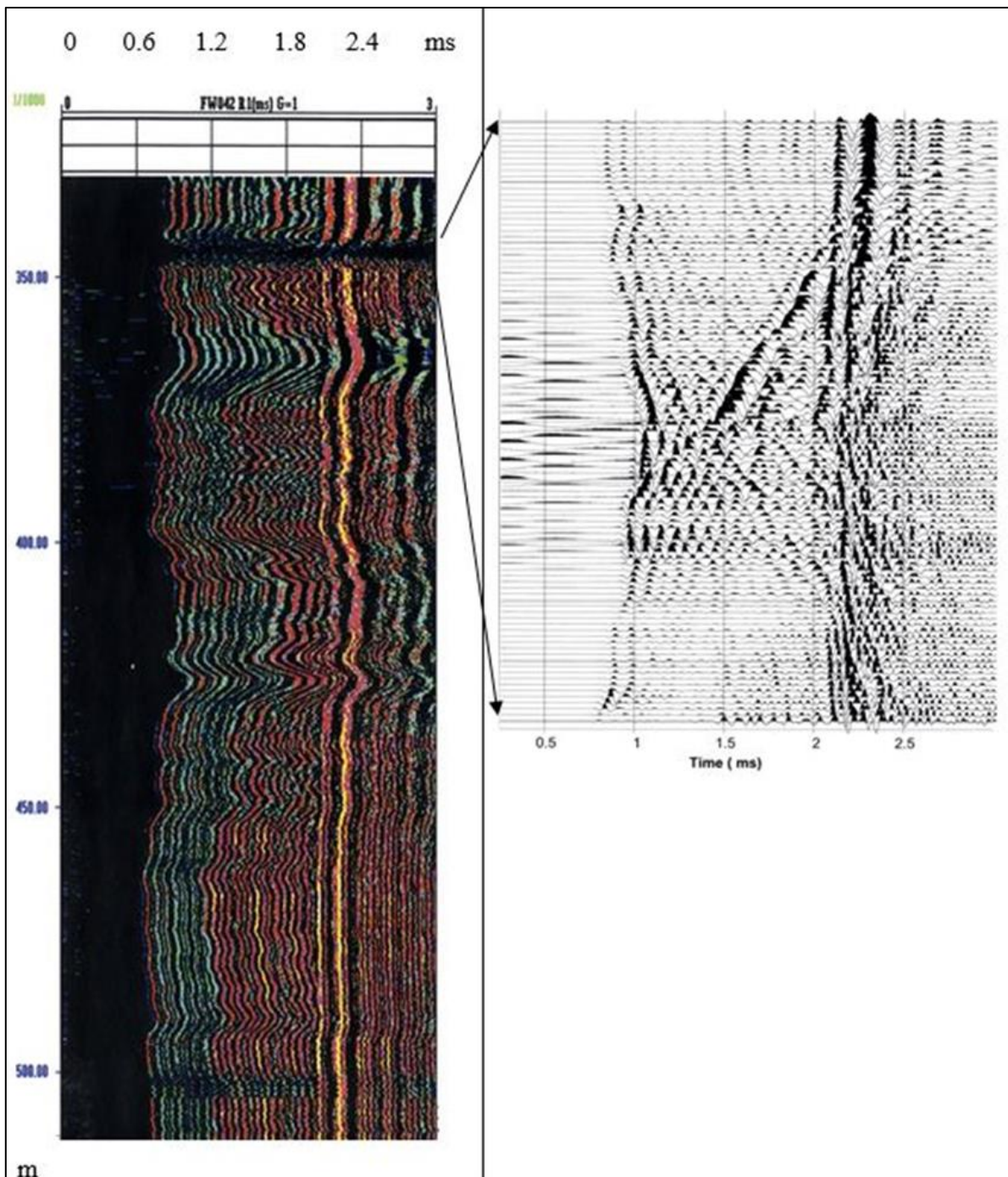


Figure 7: Acoustic logging: full waveform acoustic section (Courtesy of Andra).

Left: in the acoustic section, the refracted P-waves appear in the 0.6 – 1.2 ms time interval, the converted refracted S-waves appear in the 1.2 – 2 ms time interval. The Stoneley waves appear in the 2 – 2.4 ms time interval.

Right: Zoom in the 342 – 347 m depth interval, note the presence of criss-cross events or interfering waves.

The picked times have been used to compute the propagation velocity of the different waves and their associated correlation coefficients for editing. They

have also been used to define time windows for computing energy logs and attenuation log.

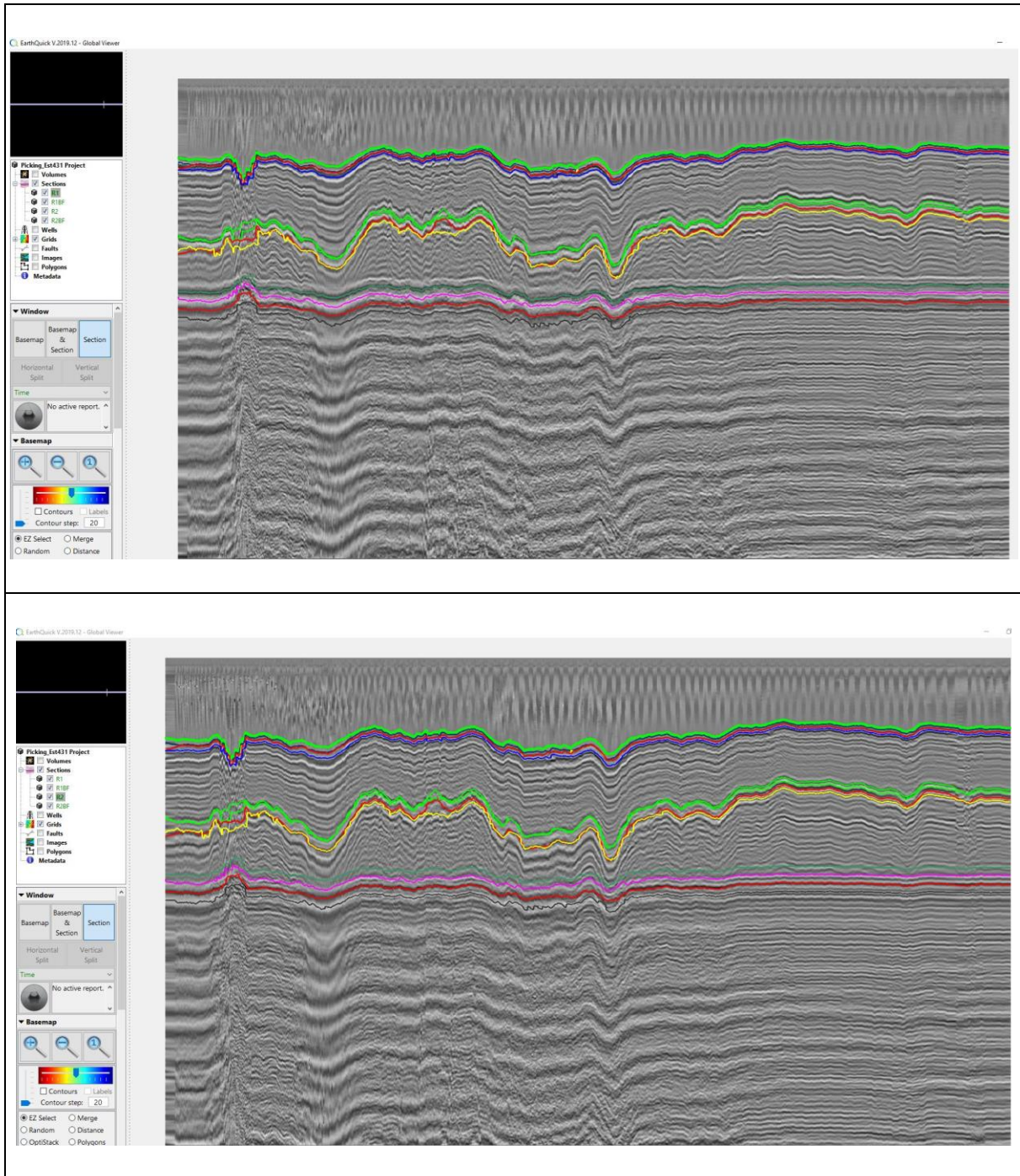


Figure 8: Acoustic sections and picked times of the different wave trains (refracted P-wave, converted refracted shear wave, Stoneley wave) with EarthQuick Software. Top: 3-m offset section (R1), Bottom; 3.25-m offset section (R2).

Figure 9 shows the results obtained for the refracted P-wave. The acoustic sections R1 (3m) and R2 (3.25 m) are muted, the acoustic signal before the arrival times of the refracted P-wave is zeroed. In a 250- $\mu$ s window after the arrival times, the correlation coefficient between the two

sections is computed at each depth in order to obtain the correlation coefficient log. A threshold of 0.85 has been introduced to edit the velocity log. More than 90 % of the measured velocities is preserved.

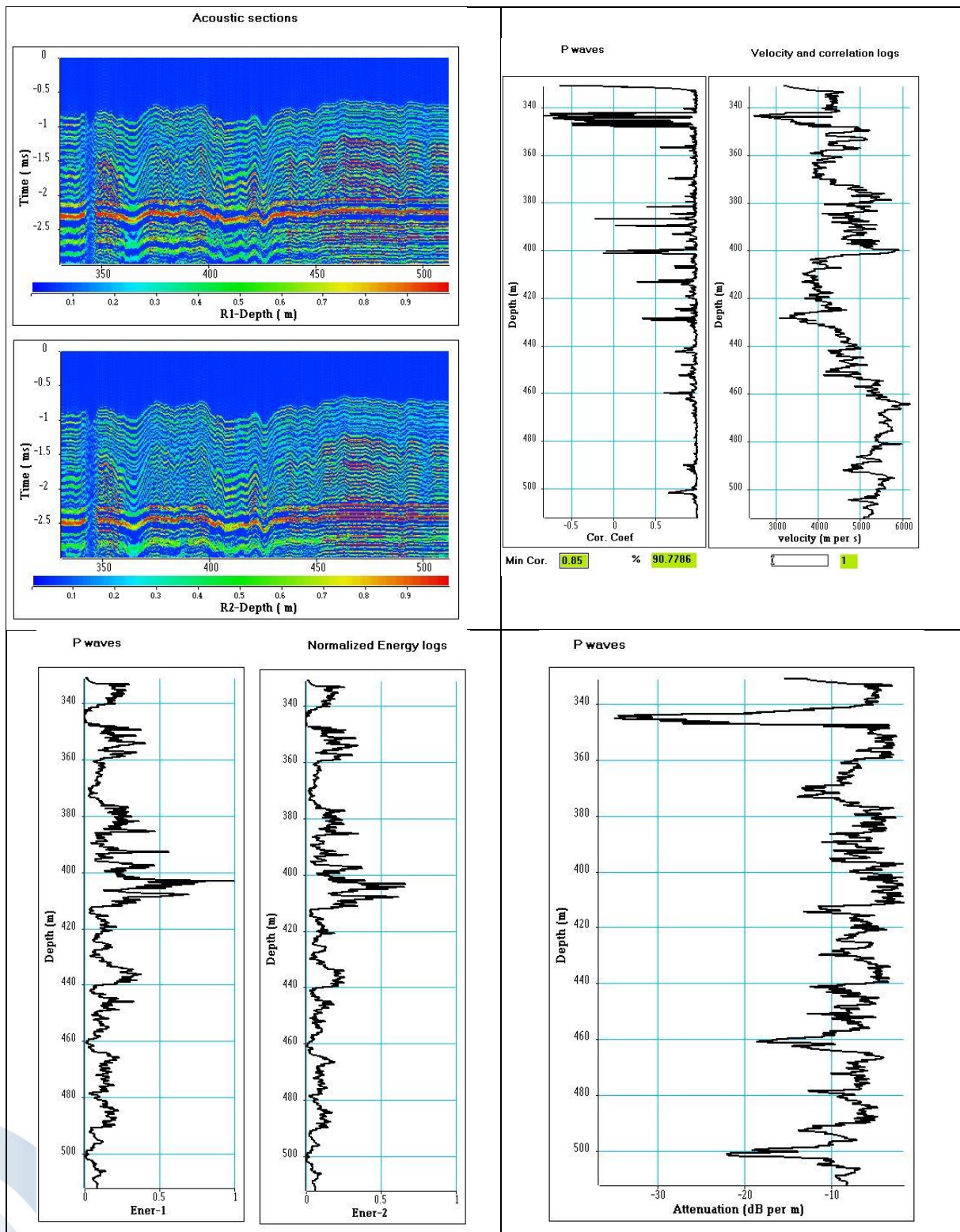


Figure 9: Refracted P-wave.

Top: acoustic sections after mute, velocity log and its associated correlation coefficient log,  
 Bottom: normalized energy logs, attenuation log.

The time windows have been also used to compute an energy log per section. The maximum of energy observed on the

section R1 is used to normalize the energy logs. The attenuation log is obtained from the ratio of the two energy logs. In the 342–

347-m depth interval, we can observe negative correlation coefficients due to the presence of interfering waves, a low energy and a strong attenuation, more than 30 dB per m.

The same procedure has been applied for the converted refracted S-wave and for the Stoneley waves. The results are shown in figures 10 and 11 respectively.

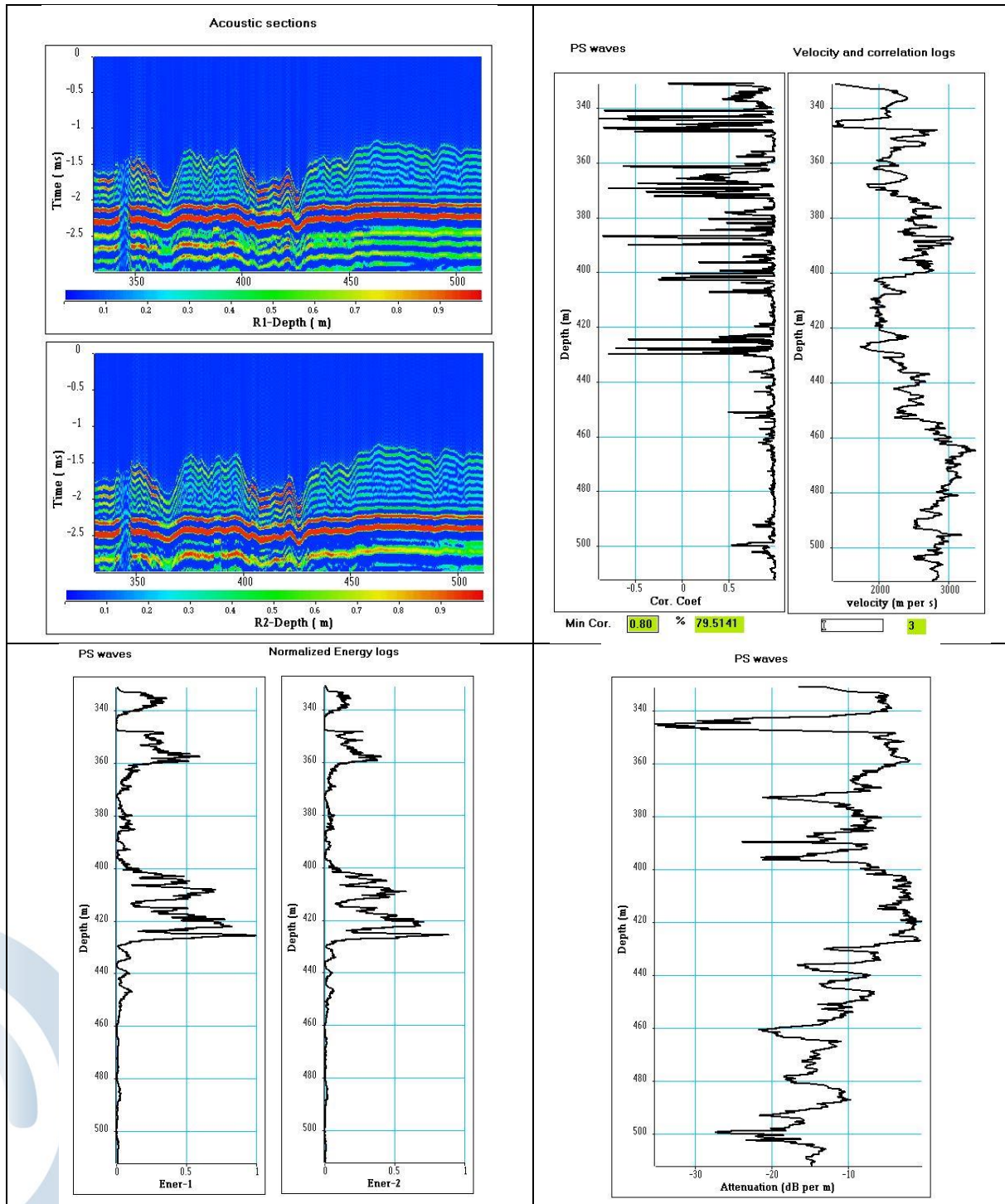


Figure 10: Converted refracted S-wave.

Top: acoustic sections after mute, velocity log and its associated correlation coefficient log, Bottom: normalized energy logs, attenuation log.

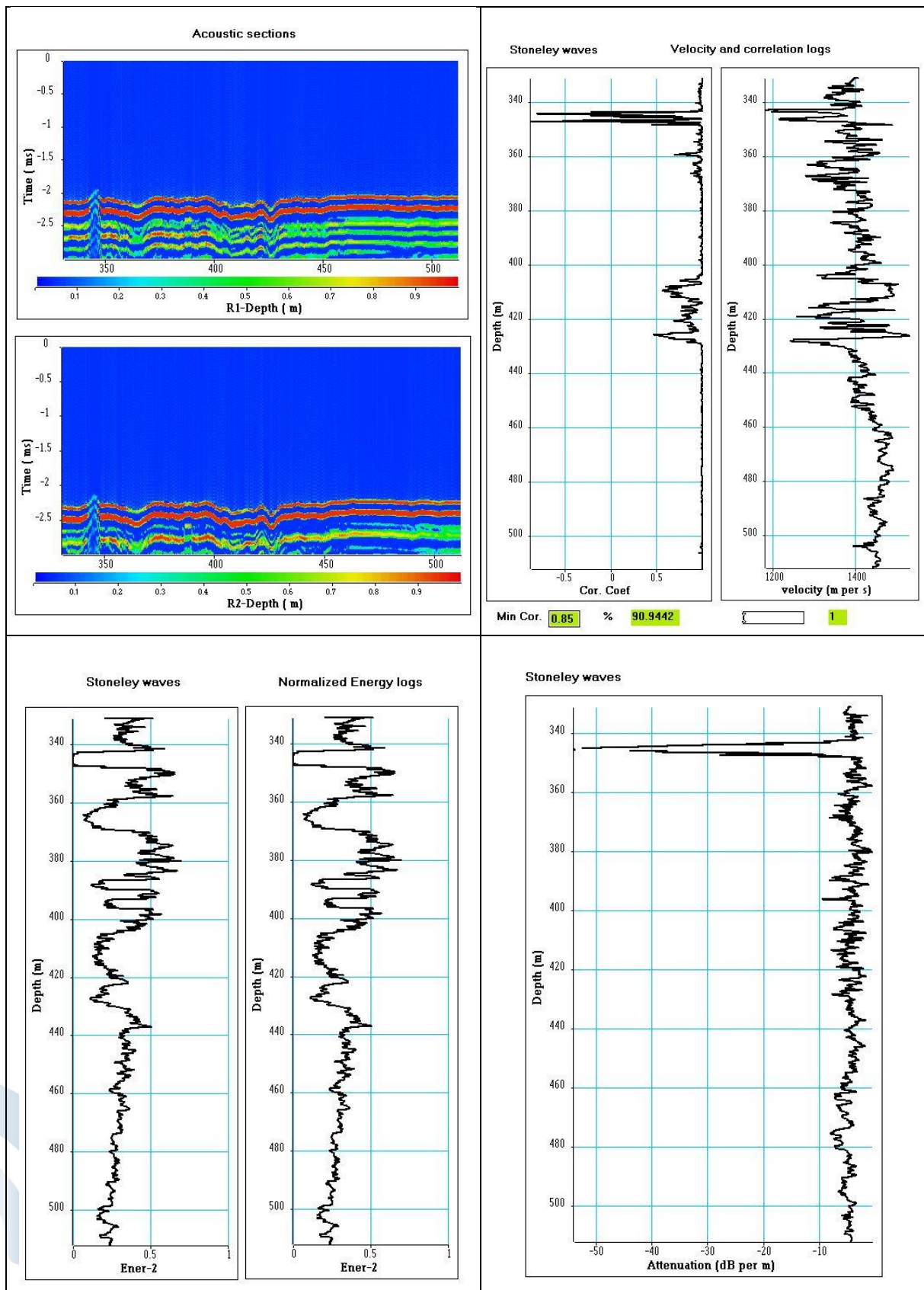


Figure 11: Stoneley wave.

Top: acoustic sections after mute, velocity log and its associated correlation coefficient log,  
 Bottom: normalized energy logs, attenuation log.

For the converted refracted S-wave, a threshold of 0.8 preserves more than 79% of the measured velocities. The energy logs and the attenuation log are computed in 350  $\mu$ s windows. A strong attenuation is measured in the 342 – 347 m depth interval.

For the Stoneley wave, a threshold of 0.85 preserves more than 90% of the measured velocities. The energy logs and the attenuation log are computed in 400- $\mu$ s windows. A strong attenuation is measured in the 342 – 347 m depth interval.

The contribution of full wave acoustic logging to the characterization of the Oxfordian formation is discussed deeply in the reference paper (J.L. Mari et al., 2011).

## Conclusions

With two field examples, we have shown that EarthQuick Software, designed for the interpretation of 2D or 3D seismic sections, can be used fruitfully in acoustic logging considering an acoustic section as a seismic section with minimum effort to load input data

Relying on a picking function of EarthQuick, an accurate picking of the arrival times of the different wave trains has been possible. That may be observed on an acoustic section: refracted P-wave, converted refracted S-wave only in fast formation and Stoneley wave in Figure 8.

The velocity logs, computed from picked arrival times of the different waves, have a higher vertical resolution than the velocity

logs obtained by semblance analysis. Furthermore, a correlation coefficient, computed in short time windows for which the start time is given by the arrival picked times of the wave under consideration, allows to evaluate the quality of the picking and to edit the velocity logs.

In the field examples, we have also shown that acoustic logging gives not only the velocities (P-wave, S-wave, Stoneley wave) of formation, but also a set of attributes such as energy logs, attenuation, Poisson's ratio, porosity... The paper mainly discusses the processing of acoustic data, but for more information on each case study it is worth referencing to the publication cited in reference.

## Acknowledgements

We thank the Cartographic and Geological Institute of Catalonia and the Instituto Geológico y Minero de España (IGME, Madrid) for granting us their permission to use the acoustic data recorded in the borehole SB-4, drilled in the northern sector of Bajo Segura Basin.

We thank Andra for granting us the permission to use the acoustic data recorded in the borehole EST431, drilled in the Oxfordian formation.

## References

- Archie, G. E. (1942). The electrical resistivity log as an aid in determining

- some reservoir characteristics, *Petroleum Technology*, 146, 54-62
- Benjumea B., López A.I., Mari J.L., García-Lobón J.L., 2019, Petrophysical characterization of carbonates (SE of Spain) through full wave acoustic data, *Journal of Applied Geophysics* 160 1-14.
  - Biot, M.A. (1956). Theory of propagation of elastic waves in a fluid-saturated porous solid, *The Journal of the Acoustical Society of America*, Vol. 28, 2, pp. 168-191.
  - Kimball, C.V., and T.L. Marzetta. (1984). Semblance processing of borehole acoustic array data, *Geophysics*, 49, 274-281.
  - Lebreton, M. and Morlier, P. (1983). Une diagraphie de perméabilité par méthode acoustique. *Bulletin of the International Association of Engineering Geology*, nº 26 – 27.
  - Mari, J.L., Gaudiani, P. and Delay, J. (2011). Characterization of geological formations by physical parameters obtained through full waveform acoustic logging, *Physics and Chemistry of the Earth*, 36, 1438-1449, Elsevier Ltd.
  - Mari J.L., López A.I., Benjumea B., García-Lobón J.L., 2018, Shape index: a refraction attribute to detect fractures and permeable bodies, paper Th J 12, 80<sup>th</sup> EAGE annual conference, 11-14 June 2018, Copenhagen, Denmark.
  - Summers G.C., Broding R.A., 1952, Continuous velocity logging, *Geophysics*, 17, 598-614.
  - White, J.E. (1965). *Seismic waves: Radiation, transmission and attenuation*. McGraw-Hill Book Compagny, New York
  - Wyllie M.R., Gregory R.J., Gardner H.F., 1956, *Elastic wave velocities in Heterogeneous and porous media*, *Geophysics*, 21, 1, 41-70.
- 